Segregation and activation of myosin IIB creates a rear in migrating cells

Miguel Vicente-Manzanares,[1] Margaret A. Koach,[1] Leanna Whitmore,[1] Marcelo L. Lamers,[2] and Alan F. Horwitz[1]

[1]Department of Cell Biology, University of Virginia, Charlottesville, VA 22908
[2]Department of Cell and Developmental Biology, Biomedical Sciences Institute, University of São Paulo SP05508-000, Brazil

We have found that MLC-dependent activation of myosin IIB in migrating cells is required to form an extended rear, which coincides with increased directional migration. Activated myosin IIB localizes prominently at the cell rear and produces large, stable actin filament bundles and adhesions, which locally inhibit protrusion and define the morphology of the tail. Myosin IIA forms de novo filaments away from the myosin IIB–enriched center and back to form regions that support protrusion. The positioning and dynamics of myosin IIA and IIB depend on the self-assembly regions in their coiled-coil C terminus. COS7 and B16 melanoma cells lack myosin IIA and IIB, respectively; and show isoform-specific front-back polarity in migrating cells. These studies demonstrate the role of MLC activation and myosin isoforms in creating a cell rear, the segregation of isoforms during filament assembly and their differential effects on adhesion and protrusion, and a key role for the noncontractile region of the isoforms in determining their localization and function.

Introduction

Cell migration is a highly regulated and coordinated process. It is comprised of several different yet integrated steps that include polarization, protrusion, and adhesion formation and turnover at the cell front, along with adhesion disassembly and tail retraction at the cell rear (Lauffenburger and Horwitz, 1996; Ridley et al., 2003). Although much is known about some of these processes, less is known about their polarization and integration. Two major and likely inter-related mechanisms contribute to establishing and maintaining polarity in migrating cells. One is through a Cdc42/aPKC/GSK/PAR6 pathway that orients the MTOC, Golgi, and nucleus (Etienne-Manneville and Hall, 2001, 2003; Gomes et al., 2005). The other is through the organization of actin, which assumes a dendritic structure that drives protrusion at the cell front, and a more filamentous, bundled structure in the cell rear (Mitchison and Cramer, 1996; Verkhovsky et al., 1999a; Pollard and Borisy, 2003).

Correlative evidence suggests that myosin II plays a role in organizing actin to establish a well-defined cell rear. It localizes in the posterior part of protruding cell fragments (Verkhovsky et al., 1999b) and the rear of motile leukocytes (Eddy et al., 2000; Xu et al., 2003), and it is excluded from lamellipodial areas in fibroblasts (Maupin et al., 1994; Kolega, 1998). In addition, myosin II is activated by phosphorylation of the myosin regulatory light chain (MLC) at the rear of the cell as a result of the activation of a RhoA/ROCK pathway (Chrzanowska-Wodnicka and Burridge, 1996), which functions in adhesion disassembly and rear retraction (Crowley and Horwitz, 1995; Burridge and Chrzanowska-Wodnicka, 1996; Worthylake et al., 2001; Ridley et al., 2003). Myosin II is also a putative downstream component of a signaling relay that includes heterotrimeric G proteins, RhoA and ROCK, and is proposed to drive the spatial segregation of the cellular poles during neutrophil chemotaxis to fMLP (Xu et al., 2003; Wong et al., 2007). Despite the evidence implicating myosin II in the formation of a cell rear, it is unclear whether it generates the cell rear or simply localizes there once a rear has formed.

Most mammalian cells express two isoforms of myosin II, myosin IIA (MIIA) and myosin IIB (MIIB), which play different but overlapping roles in the component processes of cell migration (Lo et al., 2004; Even-Ram et al., 2007; Vicente-Manzanares et al., 2007). MIIA localizes throughout the cell, including protrusions, but not at the leading edge. It is essential for the retraction of the cell edges as well as adhesion maturation at the cell front (Even-Ram et al., 2007; Vicente-Manzanares et al., 2007). MIIB also localizes in central regions and the cell rear, but not in

Correspondence to Miguel Vicente-Manzanares: mvicente@virginia.edu

Abbreviations used in this paper: FRAP, fluorescence recovery after photobleaching; MEF, mouse embryonic fibroblast; MLC, myosin light chain.

The online version of this article contains supplemental material.

The Rockefeller University Press $30.00
J. Cell Biol. Vol. 183 No. 3 543–554
www.jcb.org/cgi/doi/10.1083/jcb.200806030

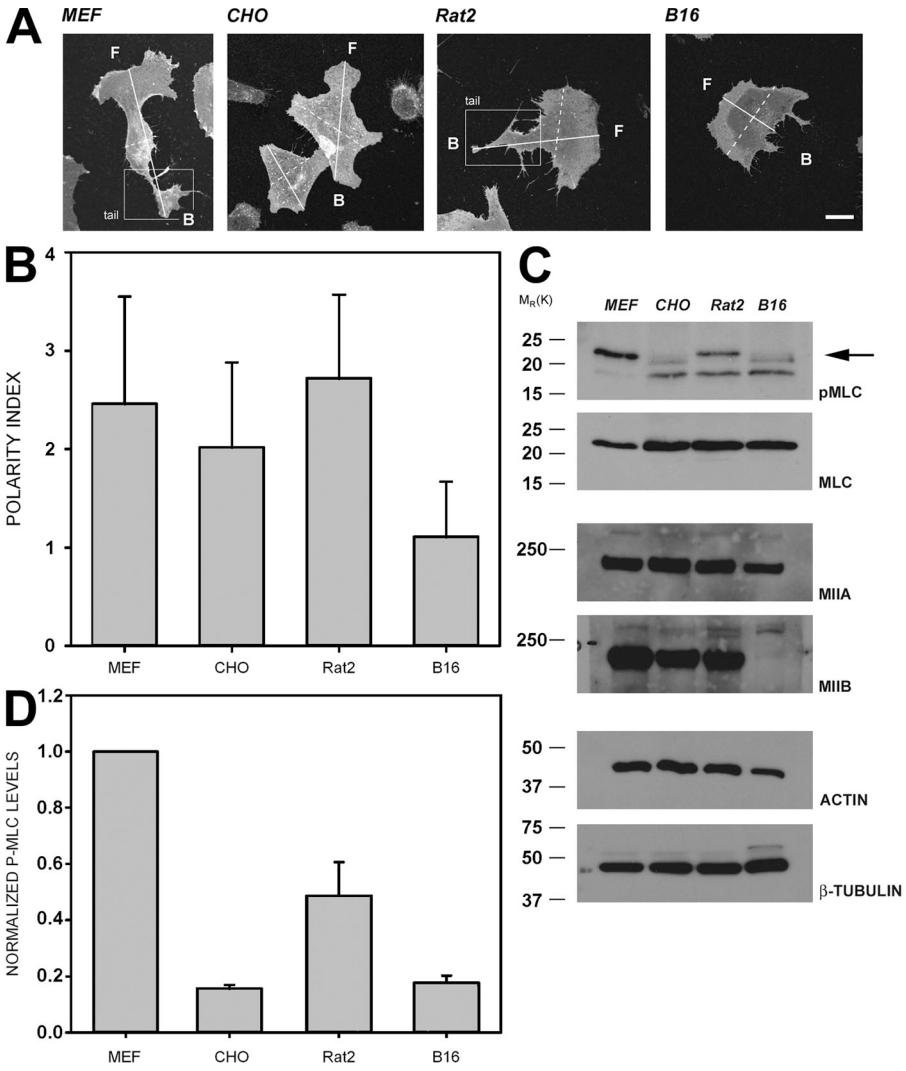

Figure 1. **A polarized morphology correlates with the amount of phosphoMLC in different cells.** (A) Representative morphologies of DiI-stained CHO.K1, MEF, B16, and Rat2 cells plated on fibronectin for 30 min. F, front; B, back. Representative axes are used to calculate the polarity index (PI) as shown in B. Solid line is the migration axis; dashed line is the transverse axis. Bar, 10 µm. (B) Polarity indices (long migratory axis divided by short transversal axis) of the cell lines shown in A under the same experimental conditions. Data represent the average ± SD of >200 cells in two independent experiments. (C) Phosphorylation of MLC and expression of myosin II heavy chain isoforms in the cell lines shown in A. The cells were plated under the same conditions. Arrow points to the P-MLC band. Representative immunoblots from four individual experiments are shown. (D) Densitometric analysis of the phosphorylation of MLC as shown in C. Values are normalized with respect to the amount of actin in control blots, and normalized values referred to the amount of P-MLC present in MEFs. Data represent the mean ± SD of four independent experiments.

protrusions. It contributes to the overall morphology of the cell as well as adhesion maturation because cells in which it is inhibited have small adhesions, assume a round morphology, and extend multiple protrusions, none of them dominant (Lo et al., 2004; Vicente-Manzanares et al., 2007). The presence and overlapping functions of these isoforms raise questions about how myosin II might contribute to the formation of a cell rear and how the two myosin II isoforms and their consequent activities become polarized.

We have used CHO.K1, COS7, and B16 melanoma cells along with mutants and chimeras of myosin II to address the role of myosin II in front-back polarization in migrating cells. We find that activated MIIB generates an extended rear by forming stable adhesions and actin bundles that do not support protrusion. MIIB binds with high affinity to these structures and assembles well away from protrusions. Conversely, MIIA assembles in anterior, protruding regions. The extended rear created by MIIB results from its C-terminal domain, where the self-assembly properties reside. Finally, MIIB activation by MLC is required for this effect. These data, in conjunction with the previous observation that MIIA alone does not generate front-back polarity (Vicente-Manzanares et al., 2007), establish a role for MIIB in creating an extended rear, or tail, lead to a model for the mechanism by which MIIB activation creates the rear, and thereby clarifies and extends previous studies implicating MII in the front-back polarity of migrating cells.

Results

Myosin II activation and actomyosin bundling induce formation of the cell rear

Myosin II and phospho-MLC localize to the back of migrating cells (Verkhovsky et al., 1999b; Eddy et al., 2000; Xu et al., 2003). To determine whether this localization causes cell polarization or is a consequence of it, we first compared the level of MLC phosphorylation in cells that exhibit a well-defined rear, or tail, with cell types in which it is poorly defined. Within 30 min after adhesion to fibronectin, mouse embryonic fibroblasts (MEFs) and Rat2 fibroblasts exhibit prominent extended rears (Fig. 1, A and B) that correlate with high levels of phosphorylated MLC (Fig. 1, C and D). In contrast, CHO K1 cells and B16 melanoma cells show localized regions of protrusion but lack an extended rear (Fig. 1, A and B); both have lower levels of MLC phosphorylation (Fig. 1, C and D). In the CHO.

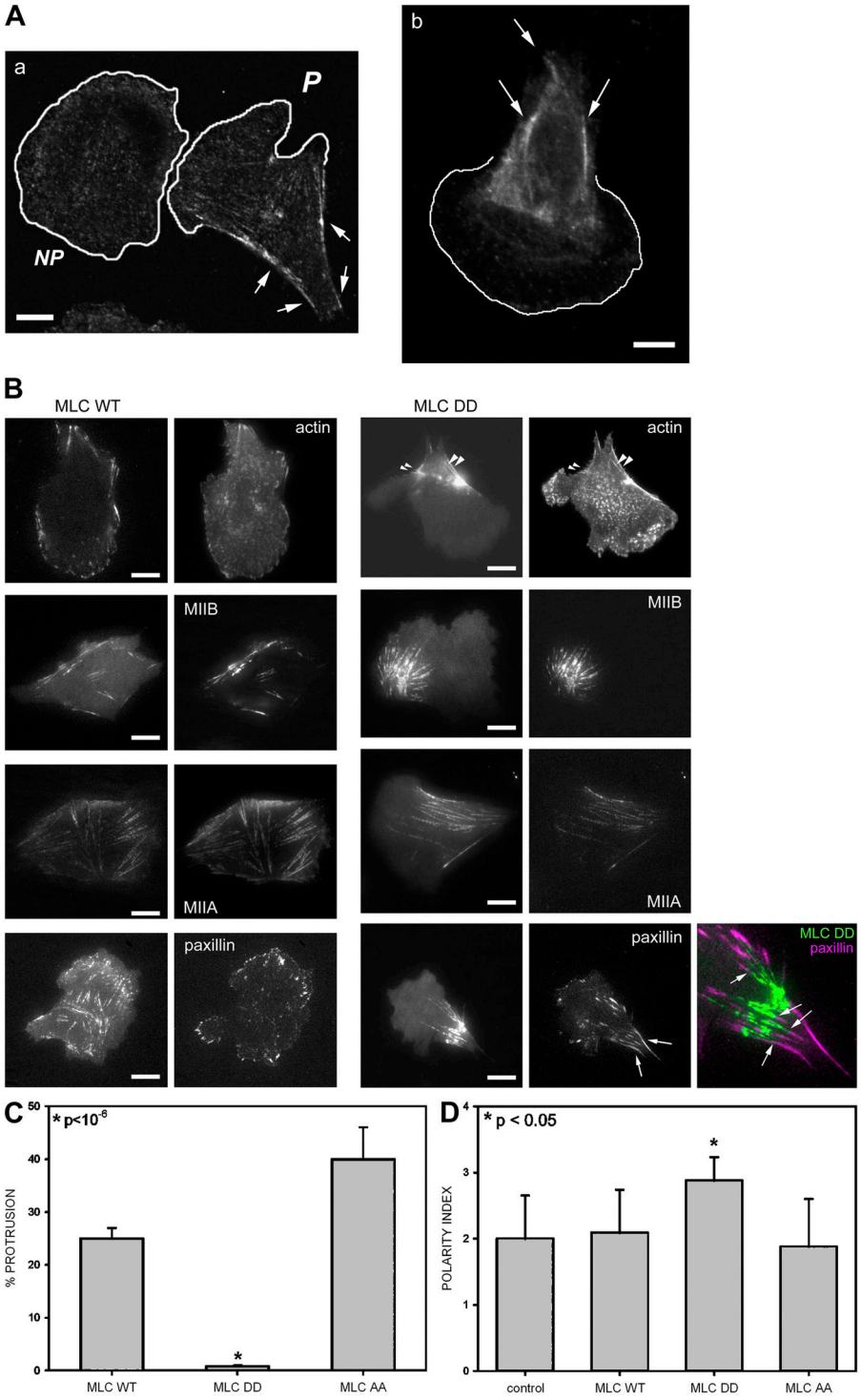

Figure 2. **Phosphomimetic MLC locally inhibits protrusion and induces formation of an extended tail.** (A) Localization of phosphorylated MLC at the rear of polarized cells. Confocal images were obtained using phosphorylated MLC antibody in polarized (P) or nonpolarized (NP) CHO.K1 cells (a) and highly polarized Rat2 cells (b). Arrows point to bundles of phosphorylated MLC at the rear. Bar, 10 µm. (B) TIRF images of CHO.K1 cells expressing wild-type MLC (left panels) or the phosphomimetic MLC-DD mutant (right panels), coexpressing actin, MIIB, MIIA, or paxillin. Bar, 10 µm. Arrowheads point to MLC-DD and actin bundles, whereas arrows point to elongated adhesions at the rear. Color inset shows a detail of the localization of paxillin (magenta) and MLC-DD. Note the almost complete lack of colocalization (arrows). Video 1 accompanies this figure and shows a cell coexpressing MLC-DD-mChe and GFP-MIIB (Video 1 available at http://www.jcb.org/cgi/content/full/jcb.200806030/DC1). (C) Effect of MLC-DD on local protrusion. CHO.K1 cells were transfected with the indicated GFP-coupled MLC mutants and mCherry to define the morphology of the cell. Protrusion was then analyzed by kymography locally in the vicinity of MLC-decorated bundles. From this, the fraction of cells showing net productive protrusion in the vicinity of the MLC bundles over 10 min was scored as a positive. Data represent the mean ± SD of >50 cells analyzed per condition in three independent experiments. *, Student's *t* test of MLC-DD vs. MLC-WT. (D) Effect of MLC-DD in cellular polarization. The polarity indices of CHO.K1 cells expressing the indicated construct were scored. Data represent the mean ± SD of >200 cells analyzed per condition in three independent experiments. *, Student's *t* test of MLC-DD vs. control/MLC-WT.

K1 cells the rear is not well defined, whereas the B16 melanoma cells show a distinct front and back; but the back is usually flat, resulting in a crescent shape. We also confirmed that B16 cells are devoid of MIIB (Fig. 1 C), as reported previously (Marigo et al., 2004), and that the other cells analyzed contained similar levels of MIIA and MIIB (Fig. 1 C, and unpublished data). Phosphorylated MLC was always excluded from lamellipodial areas, and in polarized cells it localized more prominently toward the back in well-defined bundles (Fig. 2 A). These data show a correlation between the levels of MLC phosphorylation, its location, and the formation of an extended rear.

To establish a causal role for myosin II activation in the formation of an extended rear, we expressed low levels (between 0.3 and 1.5 times that of the endogenous [Fig. S1, available at http://www.jcb.org/cgi/content/full/jcb.200806030/DC1]) of a phosphomimetic mutant of MLC, MLC-T18D,S19D (MLC-DD) in CHO.K1 cells. This mutant induced the formation of thick actin bundles, in which most of the MLC mutant colocalized with MIIA and MIIB (Fig. 2 B). Confocal as well as TIRF

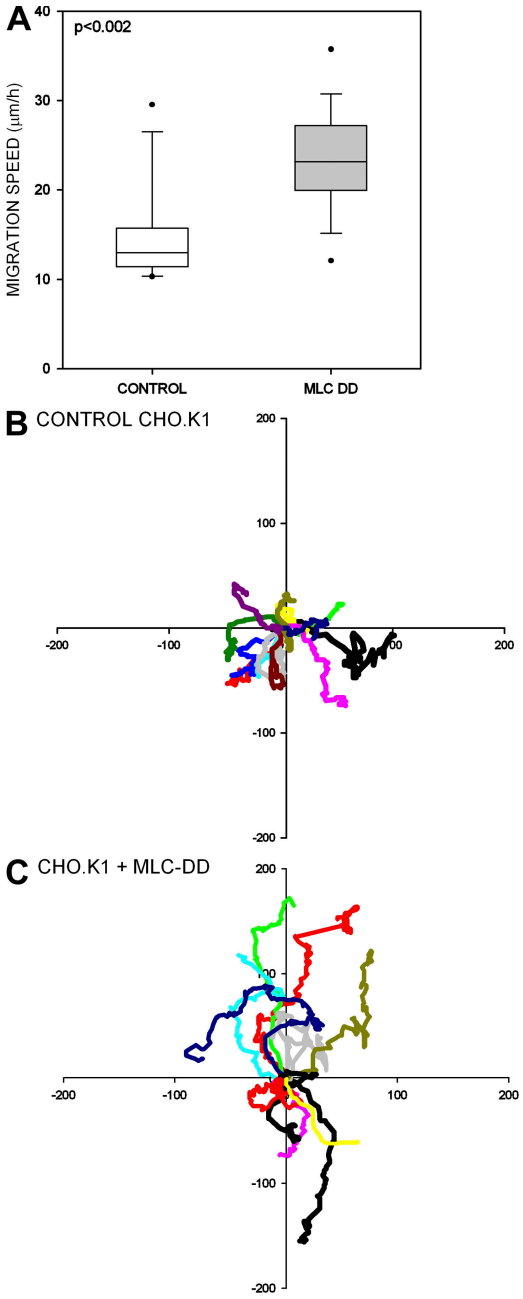

Figure 3. **MLC activation promotes cell migration.** (A) Velocities of control and MLC-DD-expressing CHO.K1 cells migrating on fibronectin. Data are box plots, which have the median value and extreme values, as well as the quartile distribution (boxed regions) of velocities of control (n = 22) and MLC-DD (n = 24) expressing cells from five independent experiments. (B and C) Migratory behavior of control (B) and MLC-DD (C) expressing CHO.K1 cells. The plots are cell tracks, derived from 6–10 h phase-contrast videos, translated to a common origin. Distance is in micrometers.

microscopy time-lapse imaging of cells expressing this mutant revealed that MLC-DD tends to concentrate in a confined region of the cell, where the actomyosin bundles accumulate (Fig. 2 B; Video 1, available at http://www.jcb.org/cgi/content/full/jcb.200806030/DC1). TIRF microscopy also showed that these actin bundles usually end in very large and elongated adhesions that are stable for at least 30 min, but they do not colocalize (Fig. 2 B, color inset). Interestingly, protrusion was inhibited in the vicinity of these MLC-DD clusters, actomyosin bundles, and large adhesions, but not in the regions of the cell distal to the large actin bundles and stable adhesions (Fig. 2 C and Video 1). Conversely, wild-type MLC or a nonphosphorylable form of MLC, MLC-AA, did not polarize or induce large, stable adhesions, and the cells protruded locally in the vicinity of MLC-decorated bundles (Fig. 2, B–D). Thus, the localized concentration of high levels of phosphorylated MLC, large adhesions, and actin bundles appears to generate a local "no-protrusion" area and an extended rear, or tail.

The formation of an extended tail produced by expression of low levels of MLC-DD increased directional migration. Both the speed (Fig. 3 A) and directionality of migration (Fig. 3, B and C) were enhanced in CHO.K1 cells expressing MLC-DD and migrating on fibronectin, compared with control cells. At higher levels of MLC-DD expression, the cells neither spread normally nor migrated, consistent with a hyper-contractile phenotype (unpublished data). These results demonstrate that formation of a stable, extended tail enhances directional migration, most likely by limiting the region of protrusion.

MLC activation creates an extended rear through its effect on MIIB

We have previously shown that CHO.K1 and Rat2 cells devoid of MIIB have a round morphology with protrusions appearing around the entire cell, rather than polarized to one region (Vicente-Manzanares et al., 2007). To determine whether the polarizing effect of MLC activation requires MIIB, we expressed the MLC-DD mutant in cells depleted of MIIB. In these cells, MLC-DD did not induce formation of a defined rear containing large stable adhesions and actin bundles as it did in control cells (unpublished data; Fig. 4, A and B), suggesting that the phosphomimetic mutant requires MIIB for its polarizing effect.

We tested this hypothesis further using B16 cells, which do not express MIIB (Marigo et al., 2004; and Fig. 1 C) and do not have an extended rear (Fig. 1 A). Expression of MLC-DD alone induces a very modest, nonstatistically significant formation of an extended rear in the B16 cells (Fig. 5 A). Furthermore, it does not localize prominently to the back of the cell; instead, it appears at the cell front (Fig. 5 A; Video 2, available at http://www.jcb.org/cgi/content/full/jcb.200806030/DC1). However, when MLC-DD and MIIB are coexpressed, the cells develop an extended rear, and both MLC-DD and MIIB localize prominently in those regions (Fig. 5, A and B). Interestingly, expression of MIIB alone does not produce a tail (Fig. 5, A and B), probably due to the low intrinsic level of MLC phosphorylation (Fig. 1 C). Together, these data demonstrate that the MLC activation induces tail formation via activation of MIIB.

Myosin IIA and IIB regulate spatially distinct phenomena in migrating cells

To further test the requirements for MIIA and MIIB in forming an extended rear and large stable adhesions (Fig. 2), we analyzed COS7 cells, which do not express MIIA (Bao et al., 2005; and Fig. S2 A, available at http://www.jcb.org/cgi/content/full/jcb.200806030/DC1). These cells generally exhibit multiple extensions of variable length (Fig. S2 B). They also rapidly extend protrusions that do not retract (Fig. S2 C, and unpublished

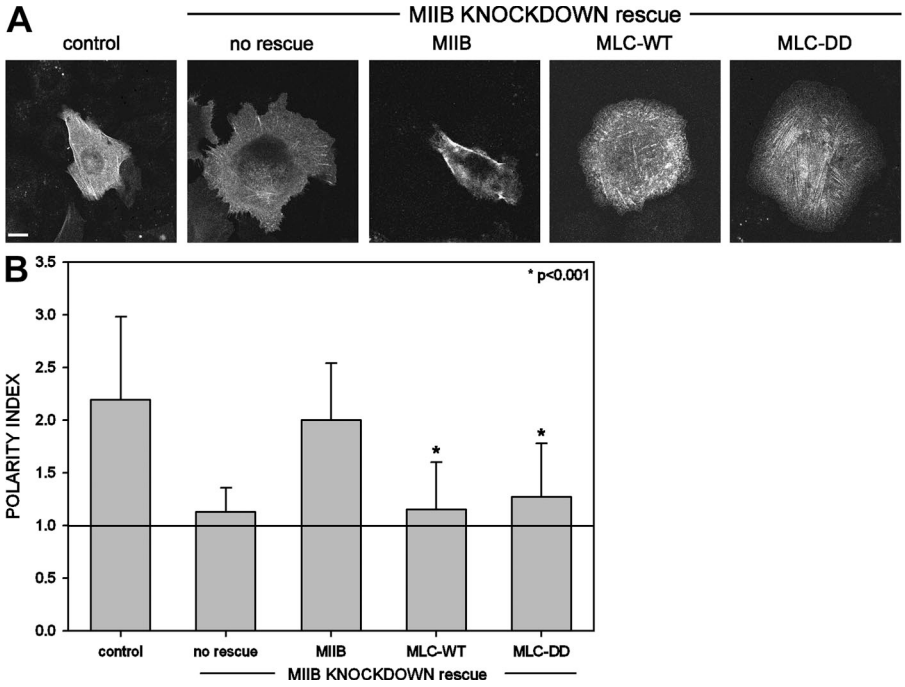

Figure 4. **MIIB creates a cellular tail.** (A) Representative images of a control or MIIB-deficient CHO.K1 cells, coexpressing control GFP-actin, RNAi-insensitive GFP-MIIB, and MLC-WT-GFP or MLC-DD-GFP. Note that MLC-DD does not rescue the polarity loss induced by depletion of MIIB. Bar, 10 µm. (B) Polarity index of CHO.K1 cells in the conditions shown in A. Data represent the mean ± SD of >100 cells analyzed per condition in four independent experiments. *, Student's *t* test of MLC-WT and MLC-DD vs. control.

data). In addition, they have inhibited adhesion maturation; e.g., few elongated, peripheral adhesions and associated α-actinin decorated actin bundles (Choi et al., 2008, Fig. S2 D, and unpublished data). When we expressed MIIA, over 60% had a single, extended rear (Fig. S2 B). In addition, the protrusion rates were reduced compared with wild-type COS7 and more typical of migrating fibroblasts (Fig. S2 C). Finally, MIIA expression produced an increase in the number of elongated adhesions and α-actinin–decorated actin bundles in protrusions (Fig. S2 E).

Localized assembly segregates myosin IIA and IIB

Because the spatial segregation of myosin IIA and B appears to determine front-rear polarity, we probed the origin of their differential localization by imaging GFP-MIIA and -MIIB in migrating CHO.K1 cells. Small clusters of MIIA appear initially in protrusions but not at the leading edge; they elongate, grow, and move retrograde as the cell moves forward (Fig. 6 A, Video 3 [available at http://www.jcb.org/cgi/content/full/jcb.200806030/DC1], and unpublished data). In contrast, MIIB

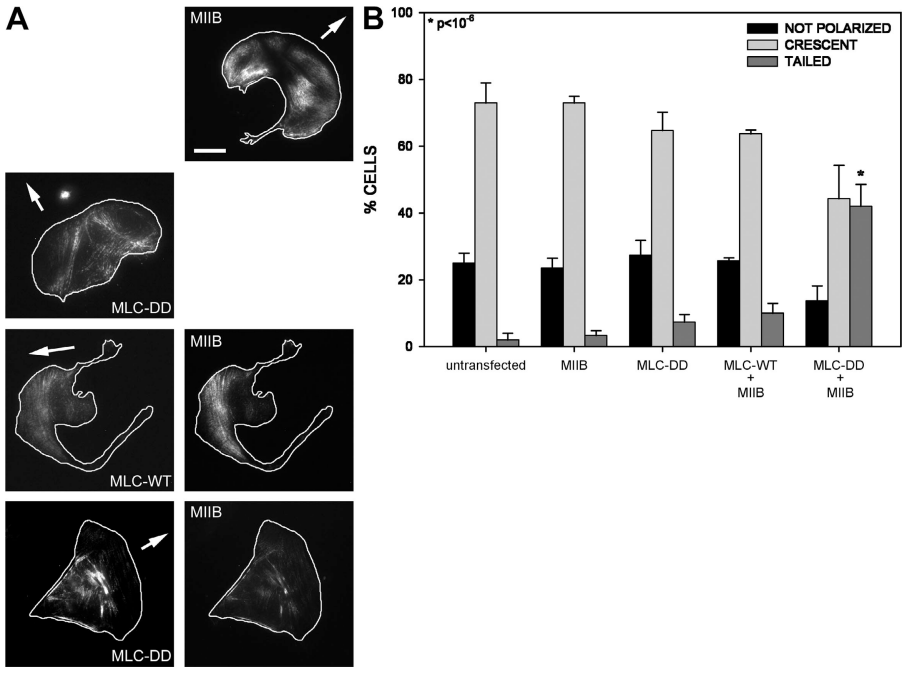

Figure 5. **MIIB activation by MLC-DD generates a cellular trailing edge.** (A) Representative images of B16 cells expressing GFP-MIIB, MLC-DD-GFP, MLC-WT-mChe + GFP-MIIB, or MLC-DD-mChe + GFP-MIIB. Bar, 10 µm. Note the formation of a robust tail in the cell expressing MLC-DD-mChe + GFP-MIIB. Video 2 accompanies this figure and represents a cell expressing MLC-DD-mChe. Note the anterior distribution of MLC-DD. (B) Quantification of the phenotypes described in A. Percentage of cells displaying the indicated morphology. Morphologies were defined as follows: "not polarized" are cells with a P.I <1.5; "crescent" are cells morphologically similar to those shown in Fig. 4 A (MIIB or MLC-DD top panels), showing a PI <1.5 and a flat or nonextended rear; "tailed" are cells with a P.I >1.5 and that show an extended rear or tail similar to the one shown in Fig. 4 A (bottom panels). Data are the mean ± SD of >300 cells per condition in two independent experiments. *, Student's *t* test of MLC-DD+MIIB vs. untransfected/MIIB alone.

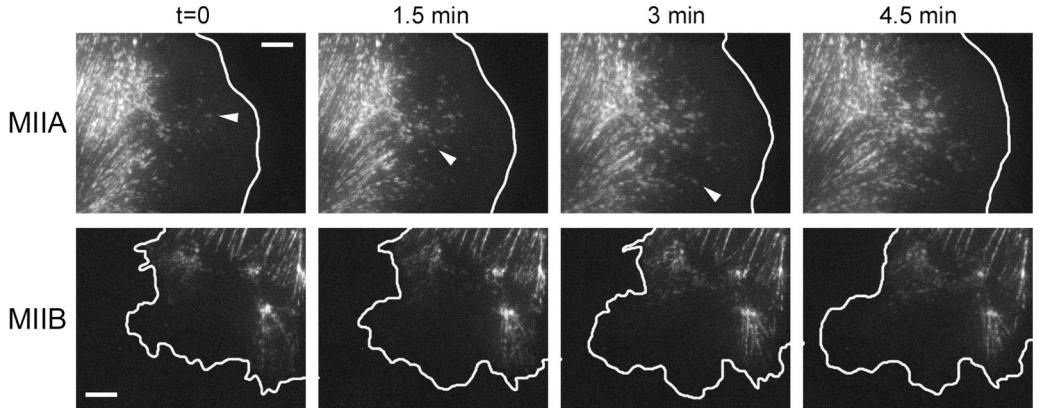

Figure 6. **The differential location of MIIA and MIIB assembly determines their subcellular localization.** (MIIA) Time-lapse sequence of a migrating CHO.K1 cell transfected with GFP-MIIA. Bar, 5 µm. Arrowheads point to representative MIIA filaments as they form. These panels correspond to Video 3 (available at http://www.jcb.org/cgi/content/full/jcb.200806030/DC1). (MIIB) Time-lapse sequence of a migrating CHO.K1 cell transfected with GFP-MIIB. Time is in minutes. Bar, 5 µm. These panels correspond to Video 4 (available at http://www.jcb.org/cgi/content/full/jcb.200806030/DC1).

seldom forms anterior clusters and tends to appear and reside in filaments away from protrusions. As the cell moves forward, this stationary region becomes the rear (Fig. 6 B and Video 4). It appears, therefore, that the critical difference between MIIA and MIIB is the ability of the former to nucleate and assemble in anterior parts of the cell. In the absence of MIIA, MIIB does not form prominent central and rear actin bundles. However, in the absence of MIIB, MIIA forms prominent filaments throughout the cell; but they are not as thick as in the control (unpublished data). This suggests that MIIA is involved in the initial formation of actomyosin bundles that emerge at the front, whereas MIIB enters subsequently as the filaments grow.

MLC activation differentially regulates the assembly of MIIA and MIIB into actomyosin filaments

We asked if MLC activation affected the segregation of the two isoforms. In wild-type CHO K1 cells, MLC-DD localizes prominently in the cell rear (Fig. 2 B). However, in the absence of MIIB, MLC-DD was distributed evenly throughout the cell, except at the tip of protrusions (Figs. 4 A and 5 A). This shows that MLC-DD acts through MIIB to generate the extended rear.

To determine whether MLC-DD associates preferentially with either isoform, we immunoprecipitated MLC-DD and immunoblotted for each isoform, and vice versa. Immunoprecipitation of MLC, or MLC-DD (Fig. S3, available at http://www.jcb.org/cgi/content/full/jcb.200806030/DC1), copurifies similar amounts of both isoforms and conversely, immunoprecipitation of either heavy chain copurifies comparable amounts of MLC (unpublished data). We also used fluorescence recovery after photobleaching (FRAP) to assess the relative affinity of MLC-DD for MIIA and MIIB using cells either depleted in or overexpressing one of the isoforms. In all cases the recovery was similar to that of the underlying MIIA or MIIB heavy chain (Fig. S4). This suggests that MLC binds to the heavy chains with a higher affinity than either of the heavy chains bind to actomyosin filaments. These data show that MLC and MLC-DD bind strongly to the underlying heavy chain and do not show a large differential preference for either isoform.

Finally, we measured the affinity of MIIA and MIIB for actomyosin filaments by measuring the FRAP of the two isoforms in the presence of the phosphomimetic mutant. MLC-DD exerted no detectable effect on MIIA recovery, whereas it inhibited the recovery of MIIB (Fig. 7, A and B). Thus, MLC activation strengthens MIIB binding to actomyosin filaments, thereby producing a more stable filament.

MIIA and MIIB segregation is regulated by their coiled-coiled domains

We then asked what intrinsic differences between MIIA and MIIB cause them to segregate. One possibility is that there are differences in the activities or affinities of their head domains; another is through differences in the self-assembly/binding properties of their C-terminal coiled-coiled domains (Egelhoff et al., 1993). To distinguish between these, we generated MIIA-MIIB head-tail domain swap chimeras: MIIA/B (head, actin-binding domain of MIIA, and tail domain of MIIB) and MIIB/A (head of MIIB and tail of MIIA) coupled to GFP and transfected them into CHO.K1 cells (Fig. 8 A). The MIIA/B chimera localized similarly to MIIB; it was excluded from protruding areas (see Fig. 10 B) and localized in the central and rear areas of the cell (Fig. 8 B). Conversely, MIIB/A localized like MIIA; it was distributed throughout the cell, except at the tip of lamellipodial extensions (Fig. 8 B; see Fig. 10 A). A similar distribution was observed when these constructs were transfected into Rat2 fibroblasts or MEFs (unpublished data).

We reported previously, using FRAP, that MIIB binds to actomyosin filaments with a higher affinity than does MIIA (Vicente-Manzanares et al., 2007). FRAP analysis on the chimeras revealed that this is also determined by the coiled domain. MIIB/A exhibited a FRAP recovery profile comparable to that of MIIA (Fig. 8 C), whereas the MIIA/B recovery was similar to that of MIIB (Fig. 8 D). Together, these data show that the localization and binding of the myosin II isoforms are dictated by the C terminus, rather than the actin-binding head domain.

To determine if localization and self-assembly properties dictated the functions of the two myosin II isoforms,

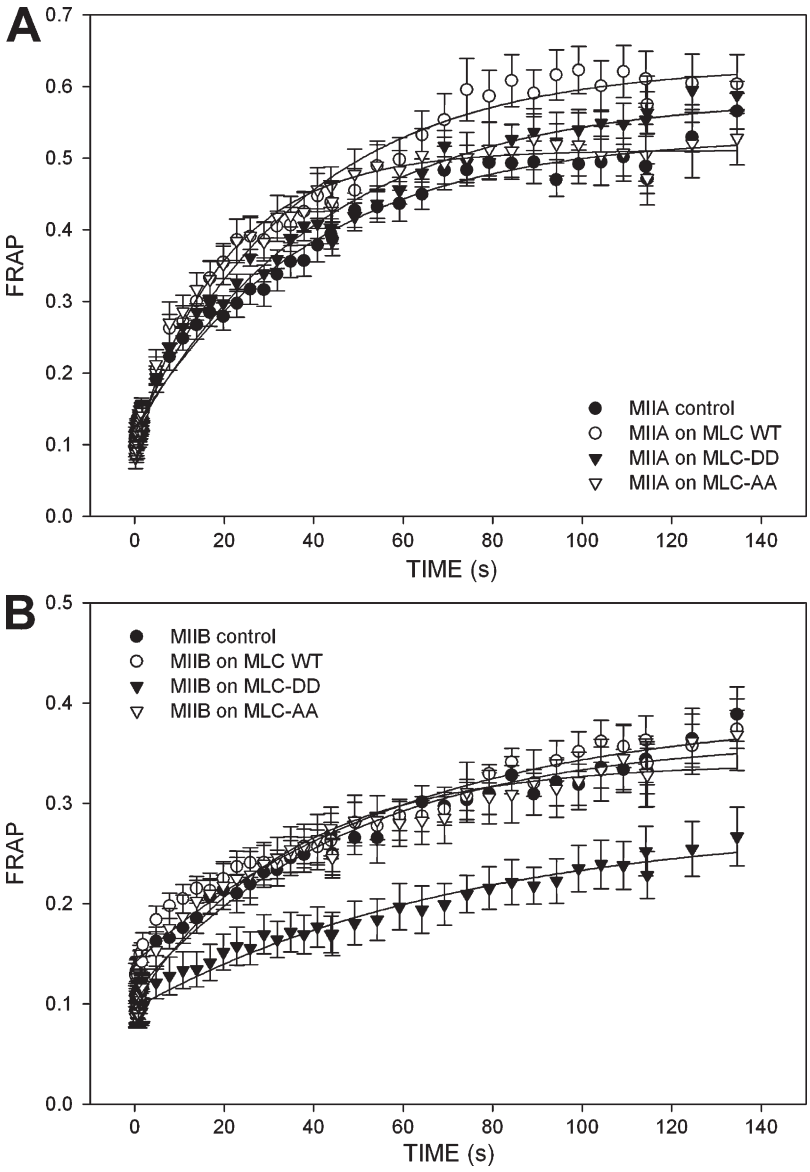

Figure 7. **MLC-DD specifically inhibits the rate of MIIB exchange from actomyosin filaments.** FRAP curves of MIIA (A) and MIIB (B) in thick actomyosin filaments, in the presence of the indicated mutants of MLC. Data are the mean ± SE of 24 individual measurements per condition in four independent experiments.

MIIB-deficient CHO.K1 cells were transfected with the two chimeras, MIIA/B and MIIB/A. Interestingly, the MIIB/A chimera did not restore front-back polarization; most cells remained round and produced lamellipodia along the entire periphery (Fig. 9 and unpublished data). Conversely, the MIIA/B chimera produced morphologies similar to those observed when the knockdown was rescued with GFP-MIIB (Fig. 9). In addition to the effects on morphology, the tail domain also rescued other aspects of MIIA and MIIB knockdowns. For example, the inhibition of adhesion maturation produced by MIIA deficiency was rescued specifically by MIIB/A (Fig. 10, A and B; Videos 5 and 6, available at http://www.jcb.org/cgi/content/full/jcb.200806030/DC1). In addition, GFP-MIIA/B rescued the multinucleation induced by MIIB deficiency (Bao et al., 2005; unpublished data).

Together, these data establish that the tail domains dictate the functional specificities of the myosin II isoforms, pointing to a prominent role of the self-assembly property of these molecules in their cellular functions.

Discussion

Our observations provide new insight into the mechanism by which migrating fibroblasts generate a rear. We have previously demonstrated a role for myosin IIA and MIIB in front-back polarization (Vicente-Manzanares et al., 2007). We have extended these observations by showing that myosin IIB activation via MLC phosphorylation induces the formation of an extended rear in migrating cells. The rear appears to result from the MIIB-mediated formation of large, stable adhesions and actin bundles, which locally inhibit protrusion. Unlike MIIA, which assembles away from MIIB to form the anterior region of the cell, MIIB mainly remains in place, tightly associated with actomyosin filaments that terminate in the large, stable adhesions that comprise the tail. The formation of an extended rear is induced by expression of the phosphomimetic MLC-DD mutant. Finally, the different properties of the MII isoforms reside in the C-terminal coiled-coiled domain, which mediates myosin II dimerization, rather than in the actin binding, motor domain.

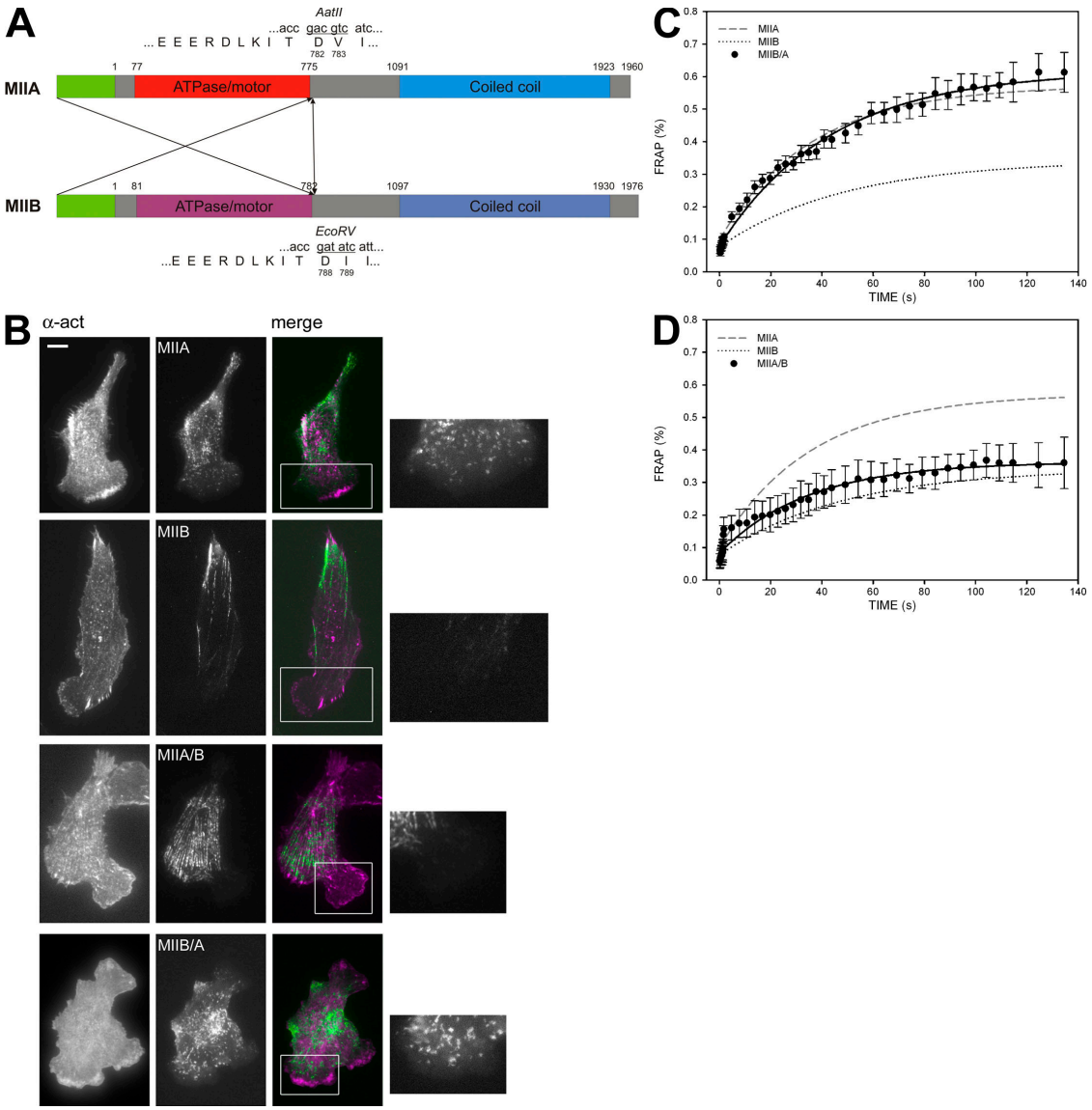

Figure 8. **The tail domain of the myosin IIA and IIB heavy chain isoforms determines the subcellular localization, polarity phenotype, and exchange rate.** (A) Cartoon depicting the domain swaps of MIIA and MIIB. Motor domains are represented in red, coiled-coil domains in blue. Unique sites used for PCR-based cloning are also shown. (B) Localization of MIIA, MIIB, and the two chimeras MIIA/B and MIIB/A. α-Actinin is used to locate the front and is shown in magenta in the colocalization panels; the myosin constructs are in green. Insets, detail of the localization of the myosin constructs in protruding areas. Note the absence of MIIB and MIIA/B in protrusions. Bar, 10 µm. (C and D) FRAP curves of MIIB/A (C) and MIIA/B (D). Average FRAP curves of wild-type MIIA and MIIB are also shown for comparison. Data are the mean ± SE of 24 individual measurements per condition in four independent experiments.

Adhesion seems to be a key player in generating cell polarity. Small, dynamic adhesions drive protrusions, whereas large, stable adhesions inhibit it (Nayal et al., 2006). Furthermore, it is generally thought that mechanical tension, induced by myosin II activation, is required for adhesion maturation and disassembly at the rear (Crowley and Horwitz, 1995; Chrzanowska-Wodnicka and Burridge, 1996). Our data suggest that an additional function of myosin II activation at the back is to create large, stable adhesions and actin bundles that locally inhibit protrusion. In addition, the formation of large adhesions at the rear of the cell is isoform dependent. MLC activation leads to the accumulation of MIIB in thick, stable actomyosin bundles. MLC has also been shown to be activated at the cell front by MLCK (Chew et al., 2002; Totsukawa et al., 2004). This activation likely promotes assembly of actin filament bundles and adhesion maturation.

The remarkable specificity of MIIB in developing a cell rear rests in its ability to form large actin filament bundles and stable adhesions ($t_{1/2}$ > 30 min). MIIB-deficient cells exhibit neither large, stable adhesions in the periphery nor large actin bundles (Vicente-Manzanares et al., 2007). Consequently, these cells do not exhibit front and back regions and appear round. Overexpression of MIIA or activation of endogenous MIIA by a phosphomimetic MLC mutant does not rescue the MIIB deficiency and the cells do not form an extended rear; however an actin-binding, but motor-inhibited, mutant of MIIB does (Vicente-Manzanares et al., 2007). This is in agreement with a recent study that shows that the contractile and cross-linking functions of myosin II cooperate to develop asymmetry in *Dictyostelium* cells (Lombardi et al., 2007), and suggests that the actin cross-linking activity of MIIB contributes to the formation

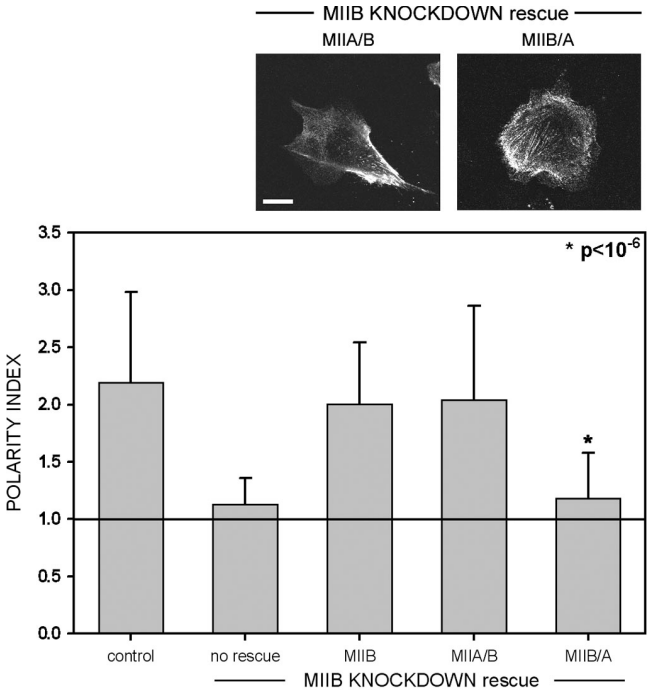

Figure 9. **Differential rescue of the MIIB-induced polarity defect by the domain swap chimeras.** MIIB knockdown cells were rescued with the indicated myosin II chimeras and plated on fibronectin. The polarity index of CHO.K1 cells was calculated as in Fig. 4. Data represent the mean ± SD of >100 cells analyzed per condition in four independent experiments. Bar, 10 µm. *, Student's *t* test of MLC-DD+GFP-MIIB/A vs. rescue with MIIB.

of the rear. However, activation of the contractile activity of MIIB (e.g., by the phosphomimetic MLC mutant) enhances this process, suggesting that MIIB contractility and actin bundling synergize to create the extended rear in migrating cells.

Myosin IIA, in contrast, is more dynamic and displays anterograde assembly and supports dynamic adhesions ($t_{1/2}$ < 10 min) and actin filaments that can disassemble to promote protrusion. It also serves in the maturation of nascent adhesions (Choi et al., 2008). Although the anterograde localization of MIIA is thought to depend on its contractile activity, which is located to the head domain (Kolega, 2006), our data suggest that it results from its self-assembly property, which resides in the coiled-coil domain. The domain swap chimera, MIIB/A that contains the coiled-coil domain of MIIA and the motor domain of MIIB behaves similarly to MIIA in terms of subcellular localization, anterograde motion, and function. Early studies identified specific phosphorylation sites on the coiled-coil domain in *Dictyostelium* myosin II that regulates self-assembly (Tan et al., 1992; Egelhoff et al., 1993). It is possible that similar regulatory sites determine the localization and function of either isoform in mammalian cells. In this regard, a recent study identified a serine residue in the tail of MIIA that could control its assembly (Dulyaninova et al., 2007), and MIIB phosphorylation is controlled by PAK (Even-Faitelson et al., 2005).

In migrating cells, the continual anterograde assembly of MIIA away from the MIIB-enriched region creates the cell front; it appears that these filaments serve as templates on which MIIB appears in the more central areas. A remaining issue, however, is what defines the initial polarity axis that determines directional migration. It is likely that the Cdc42/aPKC/GSK3/Par6 pathway does this, at least in part, by regulating MTOC and Golgi placement and nuclear translocation (Etienne-Manneville and Hall, 2001). A parallel Cdc42/MRCK pathway also involves myosin II and is required for nuclear positioning and MTOC reorientation in migrating cells (Gomes et al., 2005). Finally, our own observations point to a pivotal upstream role for MIIB in this process because its deletion results in rotating nuclei and a disorganized MTOC and Golgi apparatus (Vicente-Manzanares et al., 2007). Thus, MIIB not only creates a rear through its effect on actin and adhesion organization; but it also contributes to the overall polarity of the cell through its effects on the positioning of the MTOC and the nucleus during migration.

It is clear from the data presented here and our previous study (Vicente-Manzanares et al., 2007) that MIIB breaks the symmetry of MIIA-expressing cells to create a rear. The level of MIIB expression and activation appear to dictate the nature of the rear, which becomes extended with higher activation and expression levels. However, MIIB may not be unique in its ability to form a rear because migrating B16 melanoma cells, which have MIIC but no MIIB (Marigo et al., 2004), are crescent shaped and have a well-defined front and back. Thus, MIIB and MIIC appear to play analogous roles in creating a cell back, or rear, and thereby polarize the cell, although the nature of the back may be isoform specific.

Recently, Bourne and co-workers proposed a model for self-organizing polarity in neutrophils. This model proposes the segregation of different actin assemblies and their associated signaling ("frontness" and "backness" signals) in response to a chemoattractant gradient. These assemblies make the front more sensitive to the chemoattractant than the back (Xu et al., 2003). In this model, myosin II is thought to be a "backness" signal. Our data extend this model by invoking the different functions of the two myosin isoforms and providing a mechanism for their action. Thus, MIIB would be the target of the backness signal. MIIA, unlike MIIB, resides in anterior regions, where it supports dynamic adhesions and protrusion.

In summary, we have identified MIIB as the isoform of myosin II responsible for the generation of a well-defined tail at the cell rear during migration by creating adhesions and actin filaments that do not support adhesion turnover and protrusion. We have also shown that the two isoforms segregate based on differences in their C-terminal self-assembly domains in polarization. These domains are also largely responsible for the different properties of the two myosins; e.g., the formation of static adhesions and actin filaments for MIIB and dynamic adhesions and actin filaments that support protrusions, for MIIA.

Materials and methods

Plasmids

RNAi knockdown vectors for MIIA and MIIB have been described elsewhere (Vicente-Manzanares et al., 2007). GFP-MIIA and GFP-MIIB were a gift from Robert S. Adelstein (National Institutes of Health, Bethesda, MD; Wei and Adelstein, 2000). siRNA-insensitive GFP-MIIB and GFP-MIIB R709C have been described previously (Vicente-Manzanares et al., 2007). FLAG-MIIA and FLAG-MIIB were generated from these plasmids

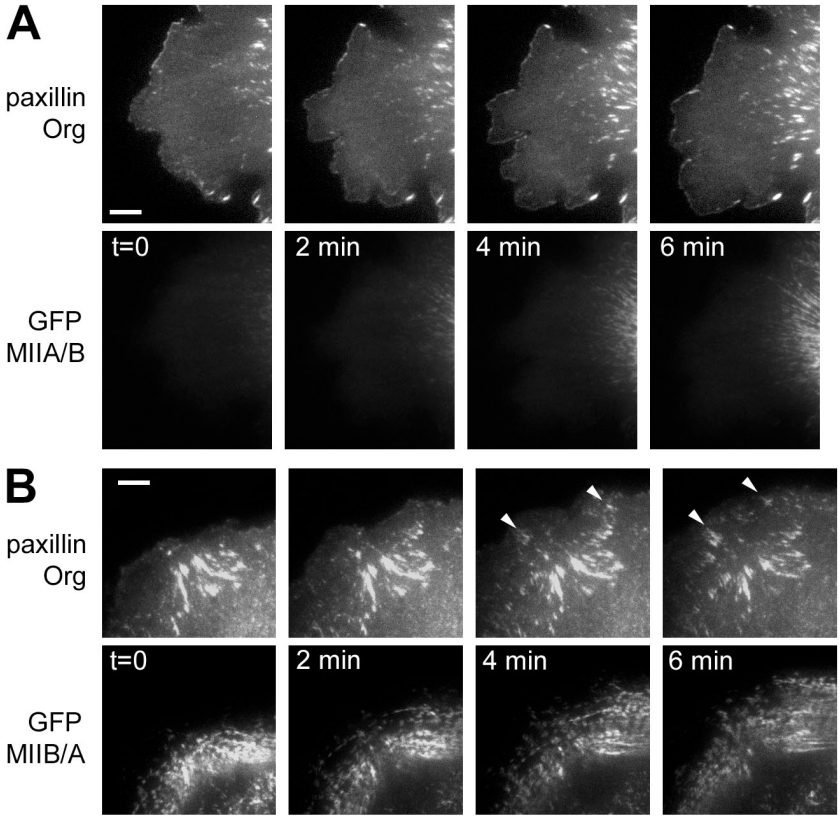

Figure 10. **The tail domain of the myosin IIA and IIB heavy chain isoforms dictates their role in adhesion dynamics.** Time-lapse sequence of protruding regions of MIIA-deficient CHO.K1 cells expressing paxillin-mOrange together with GFP-MIIA/B (A) or GFP-MIIB/A (B). Bar, 5 µm. Note the formation of elongated adhesions within the protrusion in B, marked by arrowheads, whereas the equivalent region in A remains almost devoid of large adhesions.

by substituting GFP with the FLAG epitope by PCR. MLC-GFP (MLC-WT) and MLC 18,19D-GFP (MLC-DD) were provided by Kathleen Kelly (National Cancer Institute, Bethesda, MD). MLC 18,19A-GFP (MLC-AA) was generated by site-directed mutagenesis (QuikChange, Stratagene). GFP-actin was a gift from Tim Mitchison (Harvard Medical School, Boston, MA; Watanabe and Mitchison, 2002). FLAG-MLC and FLAG-MLC 18D, 19D were subcloned into pCDNA3-FLAG2AB (Webb et al., 2005) from the GFP constructs. α-actinin–GFP and paxillin-GFP have been previously described (Laukaitis et al., 2001). GFP-vinculin was a gift from Susan Craig (The Johns Hopkins University, Baltimore, MD). Where indicated, GFP was replaced by mRFP, mCherry (mChe), from Roger Tsien (University of California, San Diego, La Jolla, CA; Shaner et al., 2004), or CoralHue monomeric Kusabira Orange (mOrange) from MBL International. GFP-MIIA/B was made by generating the N-terminal domain of MIIA by PCR, substituting the unique AatII site present in MIIA with the unique EcoRV site in MIIB (amino acids 1–783), and cloning it in-frame with the C-terminal tail of MIIB (amino acids 789–1976). The reciprocal strategy was used to generate GFP-MIIB/A. A detailed scheme is provided in Fig. 8 A.

Antibodies and reagents

The following antibodies were used: MIIA and MIIB (rabbit, pAb) from Covance; phosphorylated (T18, S19) MLC from Rockland; (mouse, IgG1); actin, from Santa Cruz Biotechnology, Inc.; β-tubulin (mouse IgG), MLC (clone MY-21, IgM), from Sigma-Aldrich.

Cell culture and transfection

MEFs (passage 4–10), CHO-K1, Rat2, COS7, and B16 melanoma cells were cultured in low- (CHO.K1) or high-glucose (MEFs, Rat2, COS7 and B16) DMEM supplemented with 10% FBS, 4 mM L-glutamine, 1 mM sodium pyruvate, 1% (vol/vol) nonessential amino acids, and penicillin/streptomycin and transfected with 0.01–0.1 µg DNA + 0.9 µg carrier plasmid (pBluescript) using Lipofectamine (Invitrogen). For knockdown experiments, plasmids containing the siRNA sequences were used in a 100:1 (1/0.01 µg, MLC constructs) or 10:1 (1/0.1 µg, other constructs) excess to GFP-, mRFP-, mCherry-, or mOrange-containing plasmids to ensure knockdown in fluorescence-positive cells. For imaging assays, cells were plated on glass-bottomed dishes, preincubated overnight with 2 µg/ml fibronectin, in CCM1 for 1 h, and maintained at 37°C at pH 7.4 (migration promoting conditions).

Immunofluorescence

Cells were allowed to adhere to fibronectin-coated coverslips (2 µg/ml) for 60 min, fixed using 4% paraformaldehyde, and permeabilized with either 0.5% Triton X-100 for 5 min or ice-cold methanol for 10 min. The coverslips were incubated with primary antibodies and a species-appropriate secondary antibody coupled to either Alexa488 or Alexa568 (Invitrogen).

Microscopy and image processing

Confocal images were collected on a microscope (Fluoview 300; Olympus) using a 60x/1.45 NA (oil) PlanApo 60xOTIRFM objective (Olympus). GFP and RFP were excited using the 488-nm laser line of an Ar ion laser and the 543-nm laser line of a He-Ne laser (Melles Griot), respectively. A Q500LP dichroic mirror (Chroma Technology) was used for GFP-labeled cells. For dual-color GFP-mRFP/mCherry/mOrange imaging, a green-red cube (488/543/633) with a DM570 dichroic mirror (Chroma Technology Corp.) was used. Fluorescence and DIC images were acquired using Fluoview software (Olympus).

TIRF images were acquired in an inverted microscope (model IX70; Olympus). The excitation laser lines used were as described for confocal microscopy. A dichroic mirror (HQ485/30) was used for GFP-labeled cells. For dual GFP- mRFP/mCherry/mOrange, a dual-emission filter (z488/543) was used. Images were acquired with a charge-coupled device camera (Retiga Exi; Qimaging) and analyzed using MetaMorph software (MDS Analytical Technologies).

Polarization assay

For Fig. 1, cells were labeled in vivo with Vybrant DiI cell-labeling solution (Invitrogen) during adhesion to fibronectin-coated coverslips, fixed, and images were acquired in a confocal microscope as described above. For each individual cell, the polarity index (PI) was calculated dividing the length of the long, migration-defined axis by the perpendicular axis passing by the centroid of the cell (see Fig. 1 for examples).

Cell migration experiments

Cells were plated on glass-bottomed dishes, preincubated overnight with 2 µg/ml fibronectin, in CCM1 for 1 h, and maintained at 37°C at pH 7.4 (migration promoting conditions). The transfected cells were identified using fluorescence for the first frame of the time-lapse video. The rest of the images were collected using very low levels of transmitted light, one image every 5 min for 6–10 h. The centroids of migrating cells were determined

using the "Manual Tracking" plugin for ImageJ, transferred, and plotted using SigmaPlot (Systat Software, Inc.). Velocities were determined as described previously (Harms et al., 2005).

Protrusiveness assay

Time-lapse videos were acquired at a frame rate of one frame/second and analyzed by kymography (Hinz et al., 1999). Regions of protrusion no farther than 3 µm away from prominent MLC clusters were used for the data in Fig. 2 C.

FRAP

Confocal images for FRAP analysis were acquired using the Olympus Fluoview 300 as described above. Initially, a cellular area (35 μm^2) that contained GFP fusion protein-decorated actin filament bundles was scanned three times, and then bleached using 15 scans at 100% laser power. To image the fluorescence recovery of fluorescence intensity after the photobleaching, we did 15 scans every 0.1 s, 15 scans every 3 s, 14 scans every 5 s, and 2 scans every 10 s. Background subtraction and normalization were calculated, and normalized intensity vs. time (sec) were fitted by a single exponential equation ($R^2 > 0.98$).

Online supplemental materials

Fig. S1 shows levels of ectopically expressed MLC-WT, MLC-DD, MIIA, and MIIB coupled to GFP. Fig. S2 shows that MIIA modulates protrusion and adhesion of MIIA-deficient COS7 cells. Fig. S3 shows biochemical interaction of MLC with MIIA and MIIB. Fig. S4 shows FRAP of the MLC-DD mutant bound to MIIA or MIIB. Video 1 shows localization and effect of MLC-DD in migrating CHO.K1 cells. Video 2 shows localization and intracellular motility of MLC-DD alone in B16 cells. Video 3 shows localization and intracellular motility of MIIA in protrusive regions of migrating CHO.K1 cells. Video 4 shows localization and intracellular motility of MIIB in protrusive regions of migrating CHO.K1 cells. Video 5 shows localization of MIIA/B in MIIA-deficient CHO.K1 cells. Video 6 shows localization of MIIB/A in MIIA-deficient CHO.K1 cells. Online supplemental materials are available at http://www.jcb.org/cgi/content/full/jcb.200806030/DC1.

We thank Robert Adelstein for the GFP-MIIA and GFP-MIIB plasmids and useful discussions, Tim Mitchison for the GFP-actin plasmid, Kathleen Kelly for the MLC-GFP plasmid, Roger Tsien for the mCherry plasmid, and Susan Craig for GFP-vinculin.

This work was supported by National Institutes of Health grant GM23244 (A.F. Horwitz).

Submitted: 4 June 2008
Accepted: 6 October 2008

References

Bao, J., S.S. Jana, and R.S. Adelstein. 2005. Vertebrate nonmuscle myosin II isoforms rescue small interfering RNA-induced defects in COS-7 cell cytokinesis. *J. Biol. Chem.* 280:19594–19599.

Burridge, K., and M. Chrzanowska-Wodnicka. 1996. Focal adhesions, contractility, and signaling. *Annu. Rev. Cell Dev. Biol.* 12:463–518.

Chew, T.L., W.A. Wolf, P.J. Gallagher, F. Matsumura, and R.L. Chisholm. 2002. A fluorescent resonant energy transfer-based biosensor reveals transient and regional myosin light chain kinase activation in lamella and cleavage furrows. *J. Cell Biol.* 156:543–553.

Choi, C.K., M. Vicente-Manzanares, J. Zareno, L.A. Whitmore, A. Mogilner, and A.R. Horwitz. 2008. Actin and [alpha]-actinin orchestrate the assembly and maturation of nascent adhesions in a myosin II motor-independent manner. *Nat. Cell Biol.* 10:1039–1050.

Chrzanowska-Wodnicka, M., and K. Burridge. 1996. Rho-stimulated contractility drives the formation of stress fibers and focal adhesions. *J. Cell Biol.* 133:1403–1415.

Crowley, E., and A.F. Horwitz. 1995. Tyrosine phosphorylation and cytoskeletal tension regulate the release of fibroblast adhesions. *J. Cell Biol.* 131:525–537.

Dulyaninova, N.G., R.P. House, V. Betapudi, and A.R. Bresnick. 2007. Myosin-IIA heavy-chain phosphorylation regulates the motility of MDA-MB-231 carcinoma cells. *Mol. Biol. Cell.* 18:3144–3155.

Eddy, R.J., L.M. Pierini, F. Matsumura, and F.R. Maxfield. 2000. Ca2+-dependent myosin II activation is required for uropod retraction during neutrophil migration. *J. Cell Sci.* 113:1287–1298.

Egelhoff, T.T., R.J. Lee, and J.A. Spudich. 1993. Dictyostelium myosin heavy chain phosphorylation sites regulate myosin filament assembly and localization in vivo. *Cell.* 75:363–371.

Etienne-Manneville, S., and A. Hall. 2001. Integrin-mediated activation of Cdc42 controls cell polarity in migrating astrocytes through PKCzeta. *Cell.* 106:489–498.

Etienne-Manneville, S., and A. Hall. 2003. Cell polarity: Par6, aPKC and cytoskeletal crosstalk. *Curr. Opin. Cell Biol.* 15:67–72.

Even-Faitelson, L., M. Rosenberg, and S. Ravid. 2005. PAK1 regulates myosin II-B phosphorylation, filament assembly, localization and cell chemotaxis. *Cell. Signal.* 17:1137–1148.

Even-Ram, S., A.D. Doyle, M.A. Conti, K. Matsumoto, R.S. Adelstein, and K.M. Yamada. 2007. Myosin IIA regulates cell motility and actomyosin-microtubule crosstalk. *Nat. Cell Biol.* 9:299–309.

Gomes, E.R., S. Jani, and G.G. Gundersen. 2005. Nuclear movement regulated by Cdc42, MRCK, myosin, and actin flow establishes MTOC polarization in migrating cells. *Cell.* 121:451–463.

Harms, B.D., G.M. Bassi, A.R. Horwitz, and D.A. Lauffenburger. 2005. Directional persistence of EGF-induced cell migration is associated with stabilization of lamellipodial protrusions. *Biophys. J.* 88:1479–1488.

Hinz, B., W. Alt, C. Johnen, V. Herzog, and H.W. Kaiser. 1999. Quantifying lamella dynamics of cultured cells by SACED, a new computer-assisted motion analysis. *Exp. Cell Res.* 251:234–243.

Kolega, J. 1998. Cytoplasmic dynamics of myosin IIA and IIB: spatial 'sorting' of isoforms in locomoting cells. *J. Cell Sci.* 111:2085–2095.

Kolega, J. 2006. The role of myosin II motor activity in distributing myosin asymmetrically and coupling protrusive activity to cell translocation. *Mol. Biol. Cell.* 17:4435–4445.

Lauffenburger, D.A., and A.F. Horwitz. 1996. Cell migration: a physically integrated molecular process. *Cell.* 84:359–369.

Laukaitis, C.M., D.J. Webb, K. Donais, and A.F. Horwitz. 2001. Differential dynamics of alpha 5 integrin, paxillin, and alpha-actinin during formation and disassembly of adhesions in migrating cells. *J. Cell Biol.* 153:1427–1440.

Lo, C.M., D.B. Buxton, G.C. Chua, M. Dembo, R.S. Adelstein, and Y.L. Wang. 2004. Nonmuscle myosin IIb is involved in the guidance of fibroblast migration. *Mol. Biol. Cell.* 15:982–989.

Lombardi, M.L., D.A. Knecht, M. Dembo, and J. Lee. 2007. Traction force microscopy in Dictyostelium reveals distinct roles for myosin II motor and actin-crosslinking activity in polarized cell movement. *J. Cell Sci.* 120:1624–1634.

Marigo, V., A. Nigro, A. Pecci, D. Montanaro, M. Di Stazio, C.L. Balduini, and A. Savoia. 2004. Correlation between the clinical phenotype of MYH9-related disease and tissue distribution of class II nonmuscle myosin heavy chains. *Genomics.* 83:1125–1133.

Maupin, P., C.L. Phillips, R.S. Adelstein, and T.D. Pollard. 1994. Differential localization of myosin-II isozymes in human cultured cells and blood cells. *J. Cell Sci.* 107(Pt 11):3077–3090.

Mitchison, T.J., and L.P. Cramer. 1996. Actin-based cell motility and cell locomotion. *Cell.* 84:371–379.

Nayal, A., D.J. Webb, C.M. Brown, E.M. Schaefer, M. Vicente-Manzanares, and A.R. Horwitz. 2006. Paxillin phosphorylation at Ser273 localizes a GIT1-PIX-PAK complex and regulates adhesion and protrusion dynamics. *J. Cell Biol.* 173:587–589.

Pollard, T.D., and G.G. Borisy. 2003. Cellular motility driven by assembly and disassembly of actin filaments. *Cell.* 112:453–465.

Ridley, A.J., M.A. Schwartz, K. Burridge, R.A. Firtel, M.H. Ginsberg, G. Borisy, J.T. Parsons, and A.R. Horwitz. 2003. Cell migration: integrating signals from front to back. *Science.* 302:1704–1709.

Shaner, N.C., R.E. Campbell, P.A. Steinbach, B.N. Giepmans, A.E. Palmer, and R.Y. Tsien. 2004. Improved monomeric red, orange and yellow fluorescent proteins derived from Discosoma sp. red fluorescent protein. *Nat. Biotechnol.* 22:1567–1572.

Tan, J.L., S. Ravid, and J.A. Spudich. 1992. Control of nonmuscle myosins by phosphorylation. *Annu. Rev. Biochem.* 61:721–759.

Totsukawa, G., Y. Wu, Y. Sasaki, D.J. Hartshorne, Y. Yamakita, S. Yamashiro, and F. Matsumura. 2004. Distinct roles of MLCK and ROCK in the regulation of membrane protrusions and focal adhesion dynamics during cell migration of fibroblasts. *J. Cell Biol.* 164:427–439.

Verkhovsky, A.B., T.M. Svitkina, and G.G. Borisy. 1999a. Network contraction model for cell translocation and retrograde flow. *Biochem. Soc. Symp.* 65:207–222.

Verkhovsky, A.B., T.M. Svitkina, and G.G. Borisy. 1999b. Self-polarization and directional motility of cytoplasm. *Curr. Biol.* 9:11–20.

Vicente-Manzanares, M., J. Zareno, L. Whitmore, C.K. Choi, and A.F. Horwitz. 2007. Regulation of protrusion, adhesion dynamics, and polarity by myosins IIA and IIB in migrating cells. *J. Cell Biol.* 176:573–580.

Watanabe, N., and T.J. Mitchison. 2002. Single-molecule speckle analysis of actin filament turnover in lamellipodia. *Science.* 295:1083–1086.

Webb, D.J., M.J. Schroeder, C.J. Brame, L. Whitmore, J. Shabanowitz, D.F. Hunt, and A.R. Horwitz. 2005. Paxillin phosphorylation sites mapped by mass spectrometry. *J. Cell Sci.* 118:4925–4929.

Wei, Q., and R.S. Adelstein. 2000. Conditional expression of a truncated fragment of nonmuscle myosin II-A alters cell shape but not cytokinesis in HeLa cells. *Mol. Biol. Cell.* 11:3617–3627.

Wong, K., A. Van Keymeulen, and H.R. Bourne. 2007. PDZRhoGEF and myosin II localize RhoA activity to the back of polarizing neutrophil-like cells. *J. Cell Biol.* 179:1141–1148.

Worthylake, R.A., S. Lemoine, J.M. Watson, and K. Burridge. 2001. RhoA is required for monocyte tail retraction during transendothelial migration. *J. Cell Biol.* 154:147–160.

Xu, J., F. Wang, A. Van Keymeulen, P. Herzmark, A. Straight, K. Kelly, Y. Takuwa, N. Sugimoto, T. Mitchison, and H.R. Bourne. 2003. Divergent signals and cytoskeletal assemblies regulate self-organizing polarity in neutrophils. *Cell.* 114:201–214.